Journal of the European Ceramic Society 40 (2020) 197–201

Contents lists available at ScienceDirect

Journal of the European Ceramic Society

journal homepage: www.elsevier.com/locate/jeurceramsoc

Short communication

Reducing the self-healing temperature of Ti_2AlC MAX phase coating by substituting Al with Sn

Zhenyu Wang[a,c], Jie Sun[d], Beibei Xu[a], Yingrui Liu[a], Peiling Ke[a,b,*], Aiying Wang[a,b,c,*]

[a] Key Laboratory of Marine Materials and Related Technologies, Zhejiang Key Laboratory of Marine Materials and Protective Technologies, Ningbo Institute of Materials Technology and Engineering, Chinese Academy of Sciences, Ningbo 315201, China
[b] Center of Materials Science and Optoelectronics Engineering, University of Chinese Academy of Sciences, Beijing, 10049, China
[c] Ningbo Institute of Industrial Technology, Chinese Academy of Sciences, China
[d] Center for Analysis and Measurements, Ningbo Institute of Materials Technology & Engineering, Chinese Academy of Sciences, Ningbo, Zhejiang, 315201, China

ARTICLE INFO

Keywords:
Ti_2AlC coating
Self-healing
MAX phase
Solid solution
Kinetics

ABSTRACT

In an effort to overcome the property degradation of Ti_2AlC MAX phase coating used in harsh environments, we fabricated a solid solution $Ti_2(Al_{0.6}Sn_{0.4})C$ coating with amount of Ti_5Sn_3 (20 wt.%) by a combined technique composing of magnetron sputtering and post-heat treatment. The cracks induced by Vickers indentation on coating surface were self-healed at 700 °C, which is the lowest self-healing temperature among the Al-based MAX phase coatings till now. The structural evolution and kinetic diffusion revealed that the formation of SnO_2 is the key factor to achieve the crack self-healing at such a low temperature for Al-based MAX phase coatings. Additionally, the self-healed $Ti_2(Al_{0.6}Sn_{0.4})C$ coating exhibited better oxidation resistance compared to the unhealed one at 800 °C. The results provide a novel and facile strategy to develop the protective MAX phase coatings with high performance at high temperature by partially substituting Al with Sn.

1. Introduction

Ti_2AlC is one of the ternary layer $M_{n+1}AX_n$ (MAX) phase ceramics, where M is an early transition metal, A is an element primarily from group 13–14, and X is either C and/or N. Such phases have attracted considerable attention due to the combined merits of high thermal conductivity, good ductility, superior high-temperature oxidation resistance, excellent corrosion resistance, as well as good irradiation resistant properties [1,2]. Such unique properties make Ti_2AlC MAX phase suitable as protective coating materials in accident tolerant fuels (ATFs) or other harsh environments [3,4]. Usually, the larger-area and thicker thermally grown Ti_2AlC coating can be obtained using a facile approach, in which the coating including Ti, Al, and C is initially deposited in appropriate content by various deposition technologies, i.e. physical vapor deposition (PVD), thermal spraying, etc, followed by heat treatment [5]. Nonetheless, common drawbacks such as cracks formed during the heat treatment and the coating growth defects (e.g. pin-holes, pores and other open voids) provide short-circuit diffusion path for the inward diffusion of corrosive particles during oxidation or corrosion processes, and thus cause severe property degradation [6,7]. Therefore, attempts to self-healing are of particular interest for enhancing the reliability and restraining these defects sensitivity of coatings.

Filling of the defects by the formation of stable oxides upon selective oxidation of Al is defined as the main self-healing mechanism for Ti_2AlC MAX phase materials, but oxidation-induced healing behavior requires high temperatures, generally over 900 °C, due to the high oxidation temperature and blunt diffusivity of the Al element [8–10]. In order to lower the self-healing temperatures of Ti_2AlC MAX phases, solid solution treatment for Ti_2AlC with Sn on the A-site would be promising because a low cohesion and migration energy as well as low-melting-point of Sn atom promotes its mobilization and oxidation at lower temperature. Bei et al. found that the oxidation temperature of Sn-containing $Ti_2(Al_{1-x}Sn_x)C$ solid solutions was reduced from 900 °C to 460 °C with increasing the Sn content [11]. In addition, the replacement of Al atoms with larger Sn atoms would increase the Ti-Al bond length in Ti_2AlC and enhance the number of vacancy sites on Al [8]. This might result in higher mobility of Al atoms, and possibly even better oxidation resistance of Ti_2AlC. However, to the best of our knowledge, the self-healing behavior of $Ti_2(Al_{1-x}Sn_x)C$ solid solutions coatings from the experimental study has not been reported till date. In this study we prepared solid solution $Ti_2(Al_{0.6}Sn_{0.4})C$ MAX phase coating and aimed to significantly lower self-healing temperature of Ti_2AlC by partially substituting Al with Sn to develop the protective MAX phase

* Corresponding author.
E-mail addresses: kepl@nimte.ac.cn (P. Ke), aywang@nimte.ac.cn (A. Wang).

https://doi.org/10.1016/j.jeurceramsoc.2019.09.009
Received 11 May 2019; Received in revised form 4 September 2019; Accepted 6 September 2019
Available online 08 September 2019
0955-2219/

coatings with high performance.

2. Experiments

The Ti-Al-Sn-C coatings were firstly deposited on the Ti6Al4V (TC4) substrates by reactive DC magnetron sputtering $Ti_{1.5}(Al_{0.5}Sn_{0.5})$ compound target in Ar/CH_4 gas precursors at a ratio of 40/1. The nominal composition of this alloy in weight per cent is: Al, 6.04; V, 4.03; Fe, 0.3; O, 0.1; N, 0.05; H, 0.015 and the balance Ti. The base pressure of the chamber was vacuumed to 3.2×10^{-3} Pa. The sputtering power was fixed at 1.6 kW and the coating was deposited for 10 h without additional heating. The annealing treatment for as-deposited coatings was applied at 750 °C in vacuum for 1.5 h to form the $Ti_2(Al, Sn)C$ MAX phase.

The crystal structure and phase formation were studied using Bruker D8 Advanced diffractometer using Cu Kα (λ = 1.5418 Å) radiation. The XRD patterns were performed using the Bruker TOPAS software to do Rietveld-refinement. Scanning Electron Microscopy (SEM, FEI Quanta 250 FEG) equipped with energy dispersive X-ray spectrometry (EDS, Oxford instrument) was used for microstructure and element mapping studies. Transmission Electron Microscope (TEM) analysis was conducted in a Talos F200 at the operating voltage of 200 keV. Cross-section TEM samples and local cross-sections were prepared by focused ion beam (FIB, Carl Zeiss, Auriga). Vickers indentation-induced cracks were in-situ healed at 700 °C in air atmosphere using an alumina tube furnace. The microstructural evolution of the crack filling with solid oxides was evaluated by SEM. The thermodynamic data for stoichiometric phase was calculated using the FactStage thermodynamic software, and if there were no thermodynamic data available for metastable phases of off-stoichiometric compositions, the Neumann-Kopp rule with linear extrapolation was used [10]. The oxidation properties of self-healed coating were tested in static air at 800 °C in alumina crucibles placed in a tube furnace. After oxidation, the oxidized samples were taken out of the furnace, and cooled down to room temperature at various intervals for mass change measurement by analytical balance. The sensitivity of the balance used for the mass measurement was 10^{-5} g. For comparison, oxidation exposures of the unhealed coating were also performed in the same tube furnace.

3. Results and discussion

The microstructure of the as-deposited Ti-Al-Sn-C coatings were characterized by TEM in cross-sectional view, as shown in Fig. 1, where a columnar structure along the growth direction of Ti-Al-Sn-C coating is evident. The selected area electron diffraction (SAED, inserted in Fig. 1a) exhibits a diffused diffraction halo, which is the typical feature of amorphous structure. Furthermore, the coating structure at a higher magnification, as presented in Fig. 1b, demonstrates that no crystallization phase is formed within the deposited Ti-Al-Sn-C coating. This can further be confirmed from the XRD patterns (see Fig. 1c), in which a broad diffraction peak at about 38° is visible. Similar results have been previously reported in the literature [12]. In addition, according to the EDS results, the atomic ratio of Ti, Al, Sn and C in the deposited coating is determined to be 52:14:14:20.

Fig. 2 shows the phase structure and microstructure of the annealed coating. After 1.5 h annealing at 750 °C, as shown in Fig. 2a, the initial columnar structure in pristine coating disappears because of the interdiffusion of elements, accompanied with the emergence of sharp crystalline diffraction rings. The typical stacking orders for the Ti_2AlC MAX phase with two TiC-slabs interleaved with a square-planar layer of Al can be seen in the HRTEM image (inserted image in Fig. 2b), when the electron beam is parallel to the [11–20] direction. The c lattice parameter deduced from the enlarged HRTEM image is 13.62 Å, a value that is in good accordance with the previous measurement [13]. From the XRD patterns of the annealed coating in Fig. 2c, the two detectable crystalline phases can be clarified to Ti_2AlC and Ti_5Sn_3, indexed by the PDF card No.29-0095 and No.10-0215, respectively. Moreover, the reflection peaks shift to small angles with the addition of Sn, which is ascribed to the increase of lattice parameters. To quantitatively identify the changes of the lattice parameters, Rietveld-refinement for the diffraction patterns was analyzed using Ti_2AlC as the structure model. To ensure the sufficient accuracy of the refinement, several refinement cycles were conducted until the final reliability factor (R-P and R-WP) was less than 10%. As shown in Table 1, the substituting content of Al with Sn and the c_0/a_0 value are determined to be 40 at.% and 4.43, respectively. The corresponding relationship between substituting content and c_0/a_0 is in line with the previous report [11], suggesting that an ideal solid solution following Vegard's law is formed in this study. The phase compositions of $Ti_2(Al_{0.6}Sn_{0.4})C$ and Ti_5Sn_3 in the coating are estimated at 80 wt.% and 20 wt.%, respectively. Meanwhile, the atomic ratio of the annealed coating is determined to be 50:14:14:22 according to the EDS results, and get close to that in the pristine coating.

The self-healing property was studied on $Ti_2(Al_{0.6}Sn_{0.4})C$ MAX phase coating containing patterns of surface cracks generated by Vickers indentation. As shown in Fig. 3a, the cracks along radial direction and axial direction are clearly distinguished after Vickers indentation, but the cracks along axial direction are wider than those along radial direction. Fig. 3b displays the secondary electron images of Vickers indentation after annealing at 700 °C for 10 h, far lower than the reported self-healing temperature of Ti_2AlC MAX phase. Obviously, the cracks are completely healed with the oxides appearing in bright contrast, and the small spherical oxides also grow where the coating defects are formed. Hence, we can conclude that both the cracks and coating growth defects are healed for the $Ti_2(Al_{0.6}Sn_{0.4})C$ MAX phase coating at 700 °C. For a detailed inspection of the reaction-formed oxides in the healed cracks, local cross-sections were made with the aids of FIB. Rectangular areas marked in Fig. 3b indicate the positions where

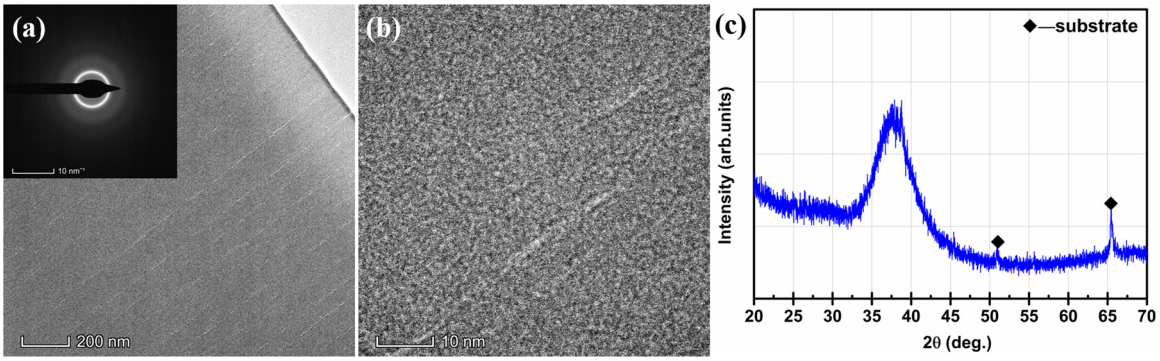

Fig. 1. TEM images and XRD patterns of the as-deposited Ti-Al-Sn-C coating. (a) Low magnification of cross-sectional view and the corresponding SAED. (b) The HRTEM image. (c) XRD patterns.

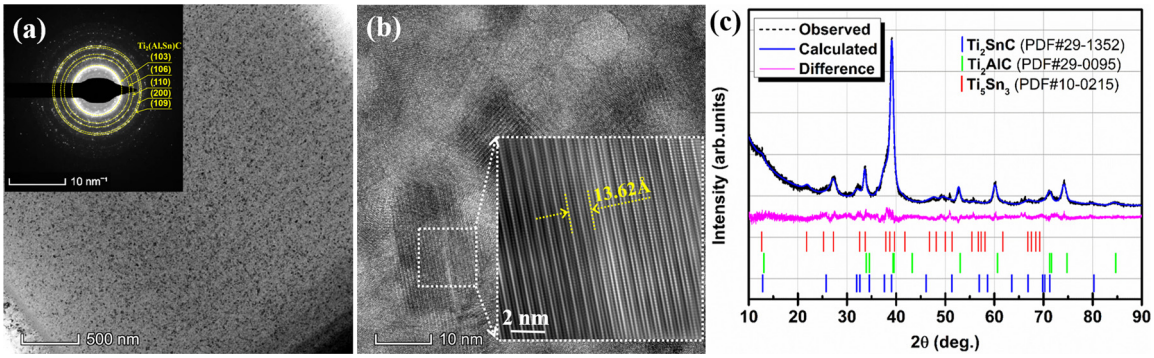

Fig. 2. TEM images and XRD patterns of the annealed Ti-Al-Sn-C coating. (a) Low magnification of cross-sectional view and the corresponding SAED. (b) The HRTEM image. (c) XRD patterns.

Table 1
Calculated phase content together with calculated lattice parameters for the annealed Ti-Al-Sn-C coating.

Phases	Content (wt.%)	a (Å)	c (Å)	c/a	R-P (%)	R-WP (%)
$Ti_2(Al_{0.6}Sn_{0.4})C$	80	3.08	13.63	4.43	3.2	7.7
Ti_5Sn_3	20	8.08	5.51	0.68		

the cross-sections are made. The SEM morphologies of the healed crack are shown in Fig. 3c-d. Apparently, the filling oxides exhibit dense structure, while the interface between the coating and oxides is not completely healed, which might be ascribed to the limited healing time. The Sn, Al, Ti and O element mapping, shown in Fig. 3e–h, reveals that the self-healing cracks are enriched in Sn, O but poor in Ti, Al. This indicates that these cracks are mainly filled with SnO_2. Further back-scatter electron image inserted in Fig. 3d verifies the filled SnO_2 oxides in the cracks exhibit bright contrast compared with other areas because backscatter electron technique reveals atomic number (Z) contrast. The self-healing phenomena are schematically illustrated in Fig. 3i.

Previous works have assumed that sufficient volume expansion upon selective oxidation of Al is a critical factor for effective self-healing of Al-based MAX phase ceramics [14]. Both theories and experiments have identified that Al in Ti_2AlC MAX phases has a high diffusion rate and activity at high temperatures due to its layered hexagonal structure with TiC-groups separated by pure Al-element layers [15,16]. The rapid diffusive mobility of Al when oxidation temperatures exceed 900 °C leads to the Al-selective oxidation, which accelerates the formation of Al_2O_3 oxides. However, achieving the self-healing at less than 900 °C for Al-based MAX phase still remains a very highly challenging task. Liu et al., [17] compared the migration energy of Al and Sn in Ti_2AC, and concluded that the diffusion migration energy of Sn in Ti_2AC with 0.66 eV is lower than that of Al with 0.83 eV. The rapid mobility of Sn driven by its fluid flow transport above its melting point of 232 °C and its low migration energy seem to favor the transportation of Sn to form Sn-oxides in oxidative atmosphere [18]. Hence, a lower oxidation temperature is to be expected for Sn when in combination with any of the shown other MAX phases, thereby decreasing the self-healing temperature by substituting Al with Sn in Ti_2AlC.

To clarify the self-healing mechanism of $Ti_2(Al_{0.6}Sn_{0.4})C$ coating, Fig. 4a shows the XRD patterns of the self-healed coating, and the calculated phase content together with calculated lattice parameters by Rietveld-refinement are listed in Table 2. X-ray peaks of rutile-TiO_2 and SnO_2 are detected after self-healing for $Ti_2(Al_{0.6}Sn_{0.4})C$ coating. From the thermodynamics, as shown in Fig. 4b, the free energies, ΔG, of SnO_2 and TiO_2 are negative, thus providing theoretical bases to understand the appearances of SnO_2 and TiO_2. The Gibbs free energy of Al_2O_3 is the lowest compared to TiO_2 and SnO_2, hence Al_2O_3 should form preferentially. However, no other peaks of Al-oxides, such as γ-Al_2O_3 and α-Al_2O_3, appear in the XRD patterns, which are ascribed to the following reasons: (1) the amount of formed Al-oxides is too small to detect within the XRD resolution limits due to its slow growth rate; (2)

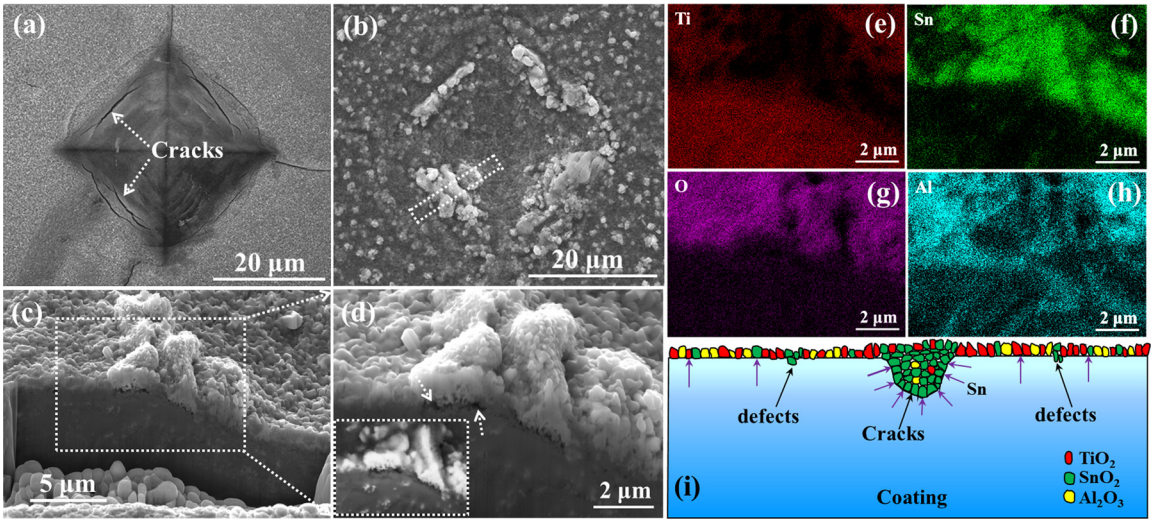

Fig. 3. (a) the cracks on the surface of $Ti_2(Al_{0.6}Sn_{0.4})C$ coating before self-healing. (b) Microstructures of the surface cracks after self-healing. (c) Low magnification image of the self-healing cracks after FIB milling. (d) An enlarged image taken from the marked area in the set of (c), the inset is the backscattered electron image. (e) Ti mapping. (f) Sn mapping. (g) O mapping. (h) Al mapping. (i) Schematic illustration of $Ti_2(Al_{0.6}Sn_{0.4})C$ coating in self-healing.

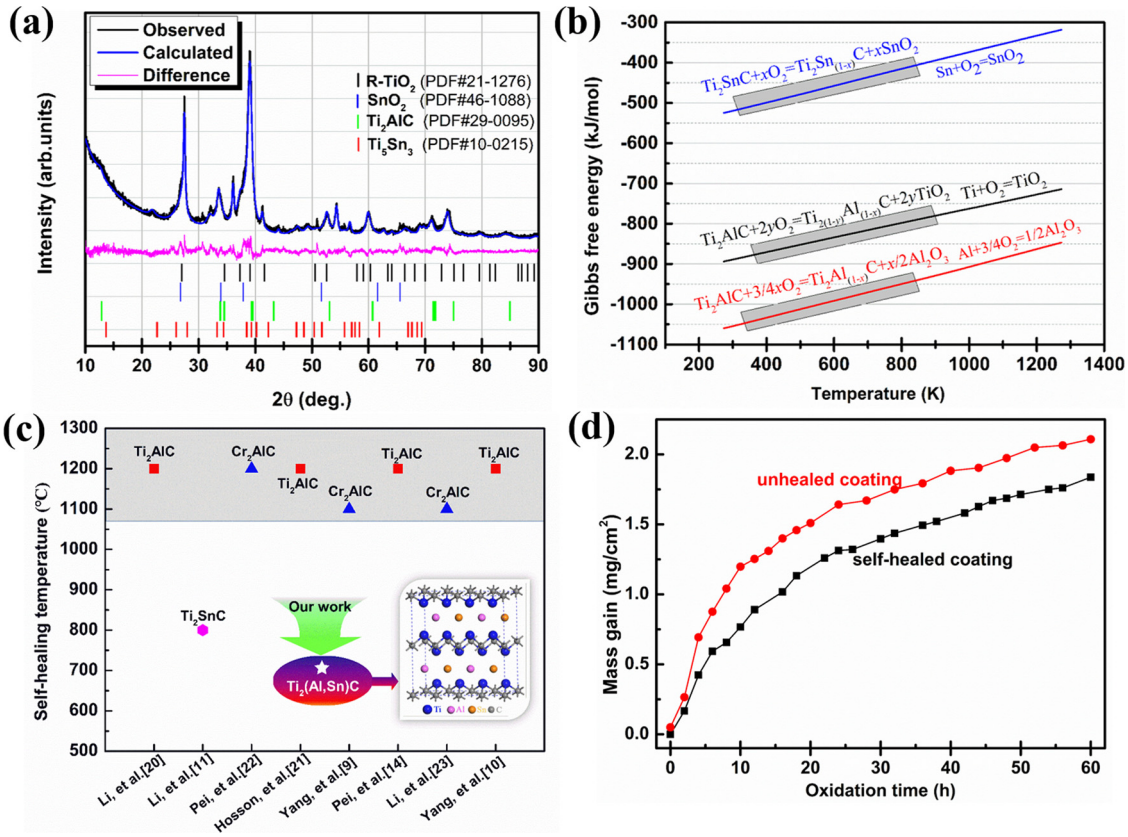

Fig. 4. (a) XRD patterns of the $Ti_2(Al_{0.6}Sn_{0.4})C$ coating after self-healing. (b) Gibbs free energy of formation of involved oxides versus temperature. (c) Comparative results of the self-healed temperatures of our work and the references. (d) The mass gains of unhealed coating and self-healed coating during oxidation at 800 °C.

Table 2
Calculated phase content together with calculated lattice parameters for self-healed coating.

Phases	Content (wt.%)	a_0 (Å)	c_0 (Å)	c_0/a_0	R-P (%)	R-WP (%)
$Ti_2(Al_{0.99}Sn_{0.01})C$	45	3.02	13.64	4.51	6.5	8.7
Ti_5Sn_3	23	8.06	5.48	0.68		
Rutile-TiO_2	23	4.59	2.97	0.65		
SnO_2	9	4.70	3.18	0.67		

these oxides exhibit amorphous or weak crystalline state. Combined with the above EDS mapping results, no aggregate phenomenon of Al around the cracks is found after self-healing. Although the content of SnO_2 (9 wt.%) is lower than TiO_2 (23 wt.%), the cracks are mainly filled by SnO_2. Therefore, thermodynamic data is considered to be insufficient to determine the formation of oxides during self-healing. The kinetics should also be among the determining factors in developing the self-healing MAX-phase materials based on thermodynamics.

In addition to TiO_2 and SnO_2, the self-healed coating is also composed of $Ti_2(Al_{0.99}Sn_{0.01})C$ MAX phase (45 wt.%) and Ti_5Sn_3 (23 wt.%). As shown in Table 2, the lattice constant of c_0/a_0 in MAX phase increases from 4.42 to 4.51 after self-healing, which contributes to the release of the Sn atoms from the MAX phase crystal lattice. Similar behavior has been found in [19] where the destabilization of Ti_2SnC crystal lattice inclines to release Sn at temperatures below 600 °C leaving a distorted $Ti_2Sn_{1-x}C$ metastable phase. In addition, the content of Ti_5Sn_3 in self-healed coating (23 wt.%) has little difference compared to the unhealed coating (20 wt.%). Therefore, it is reasonable to speculate that the oxidation of $Ti_2Al_{0.6}Sn_{0.4}C$ coating in our study enabled the self-healing to follow two stages:

$$5Ti_2Al_{0.6}Sn_{0.4}C + 2O_2 = 5Ti_2Al_{0.6}C + 2SnO_2 \quad (1)$$

$$Ti_2Al_{0.6}C + 2.95O_2 = 2TiO_2 + 0.3Al_2O_3 + CO \quad (2)$$

In contrast to the already-reported self-healing temperatures [9–11,14,21–23], as shown in Fig. 4c, the obtained solid solution $Ti_2(Al_{0.6}Sn_{0.4})C$ MAX phase coating in our study can heal the cracks induced by Vickers indentation at 700 °C, which is lowest self-healed temperature at recently, and it may be further reduced with increasing the Sn addition.

Cracks self-healing behavior of $Ti_2(Al, Sn)C$ MAX phase coating was aimed to slow the internal diffusion of corrosive particles. Therefore, the oxidation resistance properties of self-healed $Ti_2(Al, Sn)C$ MAX phase coating was studied here. The oxidation kinetics results (see Fig. 4d) indicated that the self-healed $Ti_2(Al_{0.6}Sn_{0.4})C$ MAX phase coating exhibited lower mass gains than the unhealed coating during oxidation process at 800 °C, suggesting a better protective properties. The detailed self-healing performance, including oxidation resistance mechanism, flexural strength or electrical conductivity and so on, would be discussed in our future work.

4. Conclusion

In summary, a solid solution $Ti_2(Al_{0.6}Sn_{0.4})C$ MAX phase coating with a large amount of Ti_5Sn_3 (20 wt.%) was successfully prepared by a combined technique composing of magnetron sputtering and post-heat treatment. Self-healing properties of the Vickers indentation induced cracks in $Ti_2(Al_{0.6}Sn_{0.4})C$ coating was investigated. It was found that the main healing mechanism was the filling behavior of the formed SnO_2 and some rutile-TiO_2. The most important result is that the Al-based MAX phases coating can heal coating defects (e.g. cracks, pores, etc.) even at lower temperatures of 700 °C by substituting Al with Sn having low melting point. This work is the first report of self-healing for Al-based MAX phase coatings in such a low temperature. In addition, the self-healed coating behaved lower oxidation kinetics at 800 °C

compared to unhealed coating. The achievement can provide a novel and facile strategy to fabricate outstanding MAX phase coatings with defects-free used for oxidation-/irradiation-/corrosion-resistant applications, such as the protective coatings for nuclear power plants and aerospace components.

Acknowledgements

The work was supported by the National Science and Technology Major Project (2017-VII-0012-0108), National Natural Science Foundation of China (51875555, 51901238), and Zhejiang Provincial Natural Science Foundation (LQ19E010002).

References

[1] D.J. Tallman, E.N. Hoffma, E.N. Caspi, B.L. Garcia-Diaz, G. Kohse, R.L. Sindelar, M.W. Barsoum, Effect of neutron irradiation on select MAX phases, Acta Mater. 85 (2015) 132–143.
[2] C.X. Wang, T.F. Yang, J.R. Xiao, S.S. Liu, J.M. Xue, J.Y. Wang, Q. Huang, Y.G. Wang, Irradiation-induced structural transitions in Ti_2AlC, Acta Mater. 98 (2015) 197–205.
[3] C.C. Tang, M. Steinbrueck, M. Stueber, M. Grosse, X.J. Yu, S. Ulrich, H.J. Seifert, Deposition, characterization and high-temperature steam oxidation behavior of single-phase Ti_2AlC-coated Zircaloy-4, Corros. Sci. 135 (2018) 87–98.
[4] B.R. Maier, B.L. Garcia-Diaz, B. Hauch, L.C. Olson, R.L. Sindelar, K. Sridharan, Cold spray deposition of Ti_2AlC coatings for improved nuclear fuel cladding, J. Nucl. Mater. 466 (2015) 712–717.
[5] Z.J. Feng, P.L. Ke, A.Y. Wang, Preparation of Ti_2AlC MAX phase coating by DC magnetron sputtering deposition and vacuum heat treatment, J. Mater. Sci. Technol. 31 (2015) 1193–1197.
[6] Z.J. Feng, P.K. Ke, Q. Huang, A.Y. Wang, The scaling behavior and mechanism of Ti_2AlC MAX phase coatings in air and pure water vapor, Surf. Coat. Technol. 272 (2015) 380–386.
[7] H. Yeom, B. Hauch, G.P. Cao, B. Garcia-Diaz, M. Martinez-Rodriguez, H. Colon-Mercado, L. Olson, K. Sridharan, Laser surface annealing and characterization of Ti_2AlC plasma vapor deposition coating on zirconium-alloy substrate, Thin Solid Films 615 (2016) 202–209.
[8] A.-S. Farle, C. Kwakernaak, S. van der Zwaag, W.G. Sloof, A conceptual study into the potential of $M_{n+1}AX_n$-phase ceramics for self-healing of crack damage, J. Eur. Ceram. Soc. 35 (2015) 37–45.
[9] H.J. Yang, Y.T. Pei, J.Th.M. De Hosson, Oxide-scale growth on Cr_2AlC ceramic and its consequence for self-healing, Scripta Mater. 69 (2013) 203–206.
[10] H.J. Yang, Y.T. Pei, J.C. Rao, J.Th.M. De Hosson, Self-healing performance of Ti_2AlC ceramic, J. Mater. Chem. 22 (2012) 8304.
[11] G.P. Bei, B.-J. Pedimonte, T. Fey, P. Greil, Oxidation behavior of MAX phase $Ti_2Al_{(1-x)}Sn_xC$ solid solution, J. Am. Ceram. Soc. 96 (2013) 1359–1362.
[12] Z.Y. Wang, X.W. Li, J. Zhou, P. Liu, Q. Huang, P.L. Ke, A.Y. Wang, Microstructure evolution of V–Al–C coatings synthesized from a V_2AlC compound target after vacuum annealing treatment, J. Alloys Compd. 661 (2016) 476–482.
[13] Z.J. Lin, M.J. Zhuo, Y.C. Zhou, M.S. Li, J.Y. Wang, Microstructural characterization of layered ternary Ti_2AlC, Acta Mater. 54 (2006) 1009–1015.
[14] H.J. Yang, Y.T. Pei, J.C. Rao, J.T.M. De Hosson, S.B. Li, G.M. Song, High temperature healing of Ti_2AlC: on the origin of inhomogeneous oxide scale, Scripta Mater. 65 (2011) 135–138.
[15] J.Y. Wang, Y.C. Zhou, T. Liao, J. Zhang, Z.J. Lin, A first-principles investigation of the phase stability of Ti_2AlC with Al vacancies, Scripta Mater. 58 (2008) 227–230.
[16] J.L. Smialek, Kinetic aspects of Ti_2AlC MAX phase oxidation, Oxid. Met. 83 (2015) 351–366.
[17] B. Liu, J.Y. Wang, J. Zhang, J.M. Wang, F.Z. Li, Y.C. Zhou, Theoretical investigation of A-element atom diffusion in Ti_2AlC (A = Ga, Cd, In, and Pb), Appl. Phys. Lett. 94 (2009) 181906.
[18] S.B. Li, L.Q. Zhang, W.B. Yu, Y. Zhou, Precipitation induced crack healing in a Ti_2SnC ceramic in vacuum, Ceram. Int. 43 (2017) 6963–6966.
[19] J. Zhang, B. Liu, J.Y. Wang, Y.C. Zhou, Low-temperature instability of Ti_2SnC: a combined transmission electron microscopy, differential scanning calorimetry, and x-ray diffraction investigations, J. Mater. Res. 24 (2009) 39–49.
[20] S.B. Li, G.M. Song, K. Kwakernaak, S. van der Zwaag, W.G. Sloof, Multiple crack healing of a Ti_2AlC ceramic, J. Eur. Ceram. Soc. 32 (2012) 1813–1820.
[21] H.J. Yang, Y.T. Pei, G.M. Song, J.T.M. De Hosson, Healing performance of Ti_2AlC ceramic studied with in situ microcantilever bending, J. Eur. Ceram. Soc. 33 (2013) 383–391.
[22] R. Pei, S.A. McDonald, L. Shen, S. van der Zwaag, W.G. Sloof, P.J. Withers, P.M. Mummery, Crack healing behaviour of Cr_2AlC MAX phase studied by X-ray tomography, J. Eur. Ceram. Soc. 37 (2017) 441–450.
[23] S.B. Li, L.O. Xiao, G.M. Song, X.M. Wu, W.G. Sloof, S. van der Zwaag, Oxidation and crack healing behavior of a fine-grained Cr_2AlC ceramic, J. Am. Ceram. Soc. 96 (2013) 892–899.